

tive polyketides to convert the unmodified primary PKS products into interesting metabolites.

## REFERENCES AND NOTES

- S. J. Wakil, *Biochemistry* **28**, 4523 (1989); D. O'Hagan, *The Polyketide Metabolites* (Horwood, Chichester, 1991).
- D. A. Hopwood and D. H. Sherman, *Annu. Rev. Genet.* **24**, 37 (1990); J. Robinson, *Philos. Trans. R. Soc. London Ser. B* **332**, 107 (1991); D. A. Hopwood and C. Khosla, in *Secondary Metabolites, Their Function and Evolution*, vol. 171 of the *Ciba Foundation Symposium Series* (Wiley, New York, 1992), pp. 88–112; C. R. Hutchinson *et al.*, *Actinomycetology* **6**, 49 (1992); L. Katz and S. Donadio, *Annu. Rev. Microbiol.* **47**, 875 (1993).
- J. Cortes, S. F. Haydock, G. A. Roberts, D. J. Bevitt, P. F. Leadlay, *Nature* **348**, 176 (1990); S. Donadio, M. J. Staver, J. B. McAlpine, S. J. Swanson, L. Katz, *Science* **252**, 675 (1991); D. J. MacNeil *et al.*, *Gene* **115**, 119 (1992).
- M. J. Bibb, S. Biro, H. Motamedi, J. F. Collins, C. R. Hutchinson, *EMBO J.* **8**, 2727 (1989); D. H. Sherman *et al.*, *ibid.*, p. 2717.
- M. A. Fernandez-Moreno, E. Martinez, L. Boto, D. A. Hopwood, F. Malpartida, *J. Biol. Chem.* **267**, 19278 (1992).
- M. J. Bibb, D. H. Sherman, S. Omura, D. A. Hopwood, unpublished results.
- R. McDaniel, S. Ebert-Khosla, D. A. Hopwood, C. Khosla, *J. Am. Chem. Soc.*, in press.
- D. A. Hopwood *et al.*, Eds., *Genetic Manipulation of Streptomyces: A Laboratory Manual* (John Innes Foundation, Norwich, United Kingdom, 1985); T. Kieser and D. A. Hopwood, *Methods Enzymol.* **204**, 430 (1991).
- S. P. Cole, B. A. M. Rudd, D. A. Hopwood, C. J. Chang, H. G. Floss, *J. Antibiot.* **40**, 340 (1987).
- H. L. Zhang *et al.*, *J. Org. Chem.* **55**, 1682 (1990).
- P. L. Bartel *et al.*, *J. Bacteriol.* **172**, 4816 (1990).
- F. Malpartida and D. A. Hopwood, *Nature* **309**, 462 (1984); F. Malpartida and D. A. Hopwood, *Mol. Gen. Genet.* **205**, 66 (1986).
- S. E. Hallam, F. Malpartida, D. A. Hopwood, *Gene* **74**, 305 (1988); M. A. Fernandez-Moreno, J. L. Caballero, D. A. Hopwood, F. Malpartida, *Cell* **66**, 769 (1991); J. L. Caballero, E. Martinez, F. Malpartida, D. A. Hopwood, *Mol. Gen. Genet.* **230**, 401 (1991).
- F. Malpartida, personal communication.
- K. F. Chater, in *Secondary Metabolites, Their Function and Evolution*, vol. 171 of the *Ciba Foundation Symposium Series* (Wiley, New York, 1992), pp. 144–162.
- H. C. Gramajo, E. Takano, M. J. Bibb, *Mol. Microbiol.* **7**, 837 (1993).
- The expression vector pRM5 lacks the *par* locus of SCP2<sup>+</sup>; as a result the plasmid is slightly unstable (~2% loss, as measured by one round of plating in the absence of thiostrepton). This feature was deliberately introduced in order to allow for rapid confirmation that a phenotype of interest was specified by the plasmids.
- In most naturally occurring aromatic polyketide synthase gene clusters in actinomycetes [see, for example, (4–6)], ORF1 and ORF2 are translationally coupled, with a (weak) RBS for ORF2 within the ORF1 coding sequence. In order to facilitate construction of recombinant PKSs, the ORF1 and ORF2 alleles used here were cloned as independent (uncoupled) cassettes, each with a discrete RBS. For *act* ORF1, the following sequence was engineered into pRM5: **CCACCGGACGAACGCATCG**ATTAA-TT AAgggaggACCATCATG, where the boldfaced sequence corresponds to upstream DNA from the *act*1 region, TTAATTA is the Pac I recognition site, ATG is the start codon of *act* ORF1, and the lower case letters denote the RBS. The following sequence was engineered between *act* ORF1 and ORF2: NITGAATGCATggaggAGCCATCATG, where TGA and ATG are the stop and start codons of ORF1 and ORF2, respectively, ATGCAT is the Nsi I recognition site, and the replacement of N (A in *act* DNA, A or G in alleles from other PKSs) with a C results in translational decoupling. The following sequence was engineered downstream of *act*1 ORF2: TAATCTAGA, where TAA is the stop codon, and TCTAGA is the Xba I recognition site. This allowed fusion of *act* ORF1 + ORF2 (engineered as above) to an Xba I site that had been engineered upstream of *act* ORF3 (20). As a control, pRM2 was constructed, identical to pRM5, but lacking any of the engineered sequences, so that ORF1 and ORF2 are translationally coupled. Comparison of the product profiles of CH999/pRM2 and CH999/pRM5 revealed that the decoupling strategy described here had no detectable influence on product distribution or levels.
- D. H. Sherman, E. S. Kim, M. J. Bibb, D. A. Hopwood, *J. Bacteriol.* **174**, 6184 (1992).
- C. Khosla, S. Ebert-Khosla, D. A. Hopwood, *Mol. Microbiol.* **6**, 3237 (1992).
- D. H. Sherman *et al.*, *Tetrahedron* **47**, 6029 (1991).
- D. W. Cameron, D. J. Deutscher, G. I. Feutrell, P. G. Griffiths, *Aust. J. Chem.* **34**, 2401 (1981); J. Krupa, H. Lessmann, H. Lackner, *Liebigs Ann. Chem.* **7**, 699, (1989).
- This molecule is not similar to any known precursors of the tetracenonycin C pathway, as described by S. Yue, H. Motamedi, E. Wendt-Pienkowski, and C. R. Hutchinson [*J. Bacteriol.* **167**, 581 (1986)].
- It is hypothesized that the ketoreduction occurs after the biosynthesis of the complete polyketide chain; see (7).
- R. G. Summers, E. Wendt-Pienkowski, H. Motamedi, C. R. Hutchinson, *J. Bacteriol.* **174**, 1810 (1992).
- T. A. Voelker *et al.*, *Science* **257**, 72 (1992).
- H. Fu and C. Khosla, unpublished results.
- F. Malpartida *et al.*, *Nature* **325**, 818 (1987).
- G. Muth, B. Nussbaumer, W. Wohleben, A. Pühler, *Mol. Gen. Genet.* **219**, 341 (1989).
- D. J. Lydiate, F. Malpartida, D. A. Hopwood, *Gene* **35**, 223 (1985).
- We thank M. J. Bibb, F. Malpartida, and D. H. Sherman for providing clones and sequence information. We also thank J. E. Bailey, M. J. Bibb, J. I. Brauman, M. Buttner, K. F. Chater, and T. Kieser for valuable comments on the manuscript. Supported in part by grants from the National Science Foundation (BCS-9209901), the American Chemical Society (ACS-PRF 25243-G4), the American Cancer Society (IRG-32-34) to C.K., and by the Camille and Henry Dreyfus New Investigator Award to C.K. D.A.H. acknowledges financial support from the Agricultural and Food Research Council and the John Innes Foundation.

15 July 1993; accepted 12 October 1993

## A Binary Source Model for Extension-Related Magmatism in the Great Basin, Western North America

William P. Leeman\* and Dennis L. Harry

Models for extension-related magmatism based on decompression melting of asthenospheric mantle poorly simulate fluxes and bulk compositions of magmas produced during early stages of continental extension. For the Great Basin of western North America, it is proposed that magmatism proceeded in two stages, the first involving melting of lithospheric mantle sources between 40 and ~5 million years ago (Ma), followed (since ~5 Ma) by melting of upwelling asthenospheric mantle in areas where extension has exceeded about 100 percent. This transition in magma sources is diachronous, depending on initial variations in lithosphere thickness and on rates of lithospheric thinning.

Magmatism associated with lithospheric extension has been attributed to partial melting of ascending hot mantle material. Such a mechanism reasonably accounts for many aspects of magma production in regions of high extensional strain such as mid-ocean ridge spreading centers and some rifted continental margins (1–3). However, simple decompression melting is not easily reconciled with styles of magmatism characteristic of early stages of continental rifting. First, unless the lithosphere is unusually thin or an anomalous heat source is present, a significant lag time is predicted between the onset of extension and incipient magmatism because asthenospheric magma sources (for example, “dry” peridotite) must ascend to within  $\leq$  ~80 km before significant melting occurs (1). Sec-

ond, magma production rates should generally increase with time unless the rate of lithospheric thinning decreases. Third, magma compositions should reflect a progression from deep to progressively shallower depths of melt extraction. These patterns are not always observed. For example, the principal phase of Great Basin extension began at around 40 Ma, after the late Eocene global plate reorganization, and was accompanied by voluminous synextensional silicic magmatism (4).

The present Great Basin was the locus of an Andean style magmatic belt until latest Cretaceous or early Paleocene time (~60 to 70 Ma) (5). Between ~60 to 40 Ma, magmatism in this region waned and became predominantly alkalic to shoshonitic in character. Local extension began in a belt of now-exhumed metamorphic core complexes along the eastern margin of the Great Basin (6). The amount of subsequent extension across this region varies from at

Keith-Wiess Geological Laboratory, Rice University, Houston, TX 77251.

\*To whom correspondence should be addressed.

least 100% at the latitude of Las Vegas, Nevada (7), to 75% in central Nevada (8), to probably less than 40% in southern Oregon (9). P-wave and S-wave studies of mantle anisotropy suggest that the lithosphere now is at least 65 km thick over much of this region and probably closer to 80 to 100 km thick (10, 11). If extension is taken into account, the lithosphere must have been considerably thicker at 40 Ma. For a uniform vertical strain distribution and a net 75% extension, this range implies that the pre-extension lithosphere thickness was about 115 to 175 km. With such a thick lithosphere at 40 Ma there would have been insufficient headroom for ascending asthenospheric mantle to have melted substantially unless it was significantly hotter than estimated for Cenozoic hotspot sources (1). Even today, decompression melting of ascending asthenospheric mantle is likely to occur only locally beneath parts of the southernmost Great Basin (for example, the Mojave Desert region), which are characterized by high regional heat flow, attenuated crust (20 to 25 km), and presumably highly attenuated lithosphere.

The overall pattern of late Cenozoic magmatism suggests that magma production was relatively intense during the initial stages of extension and subsequently decreased in magnitude (12). Initial (late Eocene to early Oligocene) extension was accompanied by voluminous magmatism of intermediate to silicic composition (4, 13, 14). The origin of such magmas apparently includes contributions from both crustal and mantle sources (13, 15). If a significant portion of these magmas was derived by crustal anatexis, the presence at depth of a comparable volume of mantle-derived mafic magma is implied to provide the necessary heat of fusion (14–16). This in turn implies significant melting of the mantle virtually at the onset of extension. The rarity of basaltic volcanism before the middle Miocene (~17 Ma), which marked the initiation of Basin and Range block faulting and onset of flood basalt eruptions (17), may reflect inefficient ascent of relatively dense basalt through thick sialic crust. Since the middle Miocene, basaltic volcanism waned over most of the Great Basin and largely was restricted to areas undergoing active extension (18). These patterns are inconsistent with asthenospheric melting alone as the cause of high magma fluxes during incipient extension in the Great Basin.

Although little is known about compositions of early Great Basin basalts, those erupted since ~17 Ma generally varied with time from somewhat evolved tholeiitic to more alkalic variants. Geochemical characteristics of these basalts suggest that only those erupted since ~5 Ma represent melts of asthenospheric mantle, whereas the early

lavas could have been derived from lithospheric mantle sources (19). If so, such a temporal progression of melting from shallower to deeper sources is at odds with models involving decompression melting of asthenospheric mantle. In this report, we reevaluate the relation between tectonism and magmatism in the Great Basin and propose a binary lithosphere-asthenosphere melting model that can reconcile the paradoxes outlined above.

Melting of lithospheric mantle generally has been discounted on the assumption that it likely consists of refractory peridotite that cannot produce significant amounts of magma (20). We propose instead that synextensional mid-Tertiary silicic to intermediate magmatism in the Great Basin resulted from decompression melting of mafic veins or pods within dominantly peridotite lithospheric mantle. Melts produced in this way could have ascended to crustal levels and induced formation of silicic crustal melts characteristic of the early synextensional volcanism. Development of mafic melt-metasomatism before Tertiary extension is a likely consequence of vigorous and widespread Mesozoic magmatism in this region, of magmatism associated with formation of the underlying Precambrian crust, or both. The occurrence of dikes and veins of basaltic material in mantle peridotites (21–23) provides evidence that mafic magmas are quenched during passage through the upper mantle; this notion is also supported by thermal models of magma ascent (24, 25). Entrained mafic components in dikes or veins should be more readily fusible than refractory peridotitic mantle (26, 27).

We assessed the potential for partial melting in the lower lithosphere by model-

ing pressure and temperature (P-T) conditions during extension and comparing the results with empirical melting relations. The lithosphere is assumed to deform by uniform pure shear (28). For a constant rate of extension  $U_x$ , the thickness of the lithosphere at time  $t$  is given by

$$H(t) = \frac{H_0}{(1 + U_x t/L_0)} \quad (1)$$

where  $H_0$  and  $L_0$  are the initial thickness of the lithosphere and the initial width of the extending region, respectively (29). We determined temperature at a given time by solving the one-dimensional transient heat equation with an explicit finite-difference algorithm. The fourth-order Runge-Kutta method was used to step the solution forward in time. A Lagrangian formulation is used in the model to track the temperature and depth of given rock packets through time. We estimated pressure by integrating density over depth (including the effects of thermal expansion). Lateral heat transport was neglected, so the model is most applicable at the center of relatively wide regions of extension such as the Great Basin. Constant temperature boundary conditions of 0°C and 1340°C are imposed at the surface and base of the model lithosphere, respectively; these conditions favor maximum extents of melting. Actually, the base of the mechanical lithosphere may cool somewhat during extension, but its minimum temperature will be governed by interaction with convecting asthenosphere (47) that is believed to have a potential temperature of at least 1280°C (1). However, other models (not presented here) indicate that magmatic consequences are not greatly affected by this effect for moderately high extension rates ( $\geq 10$  mm/year) characteristic of the Great Basin. The physical parameters used in the model are shown in Table 1.

For this study we ran a series of models to investigate the effects of varying initial and boundary conditions including extension rate, initial lithosphere thickness, and initial temperature at the base of the lithosphere. The model shown in Fig. 1 best approximates present geologic and geophysical features of the central Great Basin (30); it assumes a thickness of 125 km for pre-extended lithosphere at 40 Ma. Before extension, adopted P-T conditions within the lithospheric mantle range from about 1.1 GPa and 585°C at the base of the crust to 3.8 GPa and 1340°C at the base of the lithosphere (uppermost solid line, Fig. 1). After 100% extension [ $\sim 100$  million years (My) for the assumed strain rate], P-T conditions range from 0.6 GPa and 545°C to 1.9 GPa and 1340°C (lowermost solid line, Fig. 1). The base of the lithosphere (which is held at a constant temperature of

**Table 1.** Physical parameters used in the model.

Parameter	Value
Initial crust thickness	40 km
Initial lithosphere thickness	125 km
Crust density	2.9 gm cm <sup>-3</sup>
Mantle density	3.33 gm cm <sup>-3</sup>
Specific heat (crust)	875 J kg <sup>-1</sup> °C <sup>-1</sup>
Specific heat (mantle)	1250 J kg <sup>-1</sup> °C <sup>-1</sup>
Thermal conductivity (crust)	2.5 W m <sup>-1</sup> °C <sup>-1</sup>
Thermal conductivity (mantle)	3.4 W m <sup>-1</sup> °C <sup>-1</sup>
Thermal expansion coefficient (crust)	2.0 × 10 <sup>-5</sup> °C <sup>-1</sup>
Thermal expansion coefficient (mantle)	2.4 × 10 <sup>-5</sup> °C <sup>-1</sup>
Crustal heat generation	2.5 × 10 <sup>-6</sup> W m <sup>-3</sup>
Initial heat generation decay depth	10 km
Initial surface heat flux	55 mW m <sup>-2</sup>
Initial mantle heat flux	30 mW m <sup>-2</sup>

1340°C during extension) follows an isothermal path of decompression from about 3.8 to 1.9 GPa (Fig. 1). The crust-mantle boundary follows a curved path of ascent as it decompresses and cools during extension.

Peridotitic lithospheric mantle is unlikely to melt during extension unless significant heat or volatile components are added. Dry solidi for such rocks (Fig. 1) exceed temperatures of 1500°C at depths near the base of the lithosphere. If the temperature there is initially ~1340°C (1), then for reasonable conductive heating models, melting will proceed only after a long delay (~20 My) even if asthenosphere temperature instantaneously rises to ~1500°C [for example, due to impingement of a mantle plume (31)]. Advective heating by mantle plume melts could accelerate lithospheric melting, but this process is unlikely if lithosphere thickness initially exceeds ~90 km (1); as we have noted above [see also (30, 32)], the lithosphere was probably too thick for this to occur. Also, as inferred from compositions of Basin and Range basalts, melting of ascending asthenosphere apparently has occurred locally only in the last 5 My (19).

Introduction of volatiles from subducted oceanic lithosphere could lower the melting temperature of lithospheric peridotite and enhance partial melting under certain conditions (see H<sub>2</sub>O- and CO<sub>2</sub>-saturated solidi, Fig. 1). Consider a P-T path for ascending CO<sub>2</sub>-rich lithospheric mantle starting at a depth of 90 km (see labeled dashed lines, Fig. 1). Before extension, this rock packet lies just above the depth of the CO<sub>2</sub>-saturated peridotite solidus; because it never crosses far into the supersolidus field, it is unlikely to produce a significant volume of synextensional magma (33). Furthermore, CO<sub>2</sub>- or H<sub>2</sub>O-saturated pyrolite compositions (Fig. 1) have unrealistically high fluid contents for most regions of the mantle. Even if the lithospheric mantle initially contained large amounts of H<sub>2</sub>O or CO<sub>2</sub> at the onset of rifting (for example, as a result of infiltration of subduction-derived melts or aqueous fluids), volatiles not bound in mineral phases could be incorporated in small-volume early melts. Melting relations for the progressively devolatilized residue would then shift toward the dry peridotite solidus, retarding further melt production unless an auxiliary source of heat or renewed volatile flux was available. For such reasons it is unlikely that the voluminous early synextensional magmatism in the Great Basin was caused by melting of peridotitic rocks anywhere in the mantle.

Phase relations for a typical basalt (Fig. 1) support an alternative scenario for lithosphere melting. The lithosphere normally is cooler than the basalt liquidus curve [1475°C at 120 km (34)]; hence, basaltic

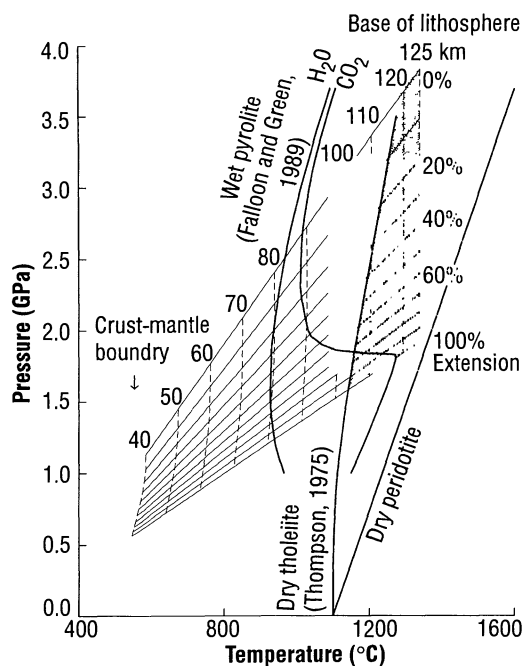


**Fig. 1.** The P-T conditions in the model lithospheric mantle during extension. Heavy solid lines indicate solidi for selected compositions, including dry and H<sub>2</sub>O- and CO<sub>2</sub>-saturated peridotite (1, 46) and a tholeiitic basalt (34). Diagonal solid lines indicate the range of P-T conditions between the base of the crust and the base of the lithosphere at the indicated percentages of extension. Dashed lines indicate P-T paths of given packets of rock during extension, with the initial depth of the rock packet indicated at the top. The shaded area represents the portion of the model lithosphere that undergoes partial melting during extension.

magmas traversing this domain will partially quench and ascend as crystal-liquid mixtures. Segregation of the liquids would leave cumulate mineral assemblages [for example, pyroxenite ± garnet (34)] as well as products of melt-wallrock reaction [pyroxenite or amphibolite ± olivine (23, 26)] in the lithospheric mantle. Ascending magmas would tend to quench entirely if they achieved thermal equilibrium with their wallrocks; this is reasonable where heat losses are large, relative to ascent velocity, as in narrow dike-like conduits (35). Thus, although the buoyancy of basaltic magmas relative to mantle lithologies favors their ascent, some of the available magma is likely to freeze within the lithosphere (25). It is widely accepted that basaltic magmas have underplated and intruded the continental crust in many tectonically active regions (36). We suggest that wherever basaltic magmatism has occurred, quenched basaltic products are important components in the lithospheric mantle as well.

Rocks of basaltic composition at the base of the lithosphere would be near their melting point before extension (~120 km for the case shown) and would begin to melt virtually at the onset of lithospheric attenuation. Because calculated ascent trajectories are nearly isothermal for the first 100% of stretching (29), melt fraction would increase with time, and high degrees of melting would be achieved near 60-km depth. However, portions of the mantle initially shallower than ~100 km never cross the dry solidus, and in this example, melt production is limited to the lowermost 20 km of the model lithosphere (Fig. 1). Furthermore, melt production proceeds up-

ward from the bottom as successively shallower rock packets ascend and cross the basalt solidus. The thickness of the portion of lithosphere undergoing partial melting increases monotonically with time, but at a decreasing rate. This process results in essentially continuous melt production from the onset of extension. Melt production is limited eventually by cooling of the ascending lithospheric mantle and by increasing refractivity of the included mafic domains as magma is extracted.

Melt production from a mafic source rock was estimated with a linear relation between melt fraction and excess temperature above the solidus on the basis of experimental studies of a dry tholeiitic basalt (37). This simple model ignores the effect of melt extraction in modifying the bulk composition of the residue or its subsequent melting behavior, details that cannot be resolved without appropriate experimental studies. A more detailed analysis of melting seems unwarranted in view of such uncertainties. Melt compositions are expected to range from relatively siliceous to basaltic with increasing melt fraction (34). Thus, the inferred presence of voluminous mafic magmas during early rifting stages requires relatively high degrees of melting of basaltic source components; more mafic source rocks (such as pyroxenite) could produce initial melts that approach basaltic compositions at lower melt fractions, albeit at higher temperatures. Alternatively, some of the predominantly intermediate to silicic early synextensional magmas could be produced as partial melts of mafic protoliths in the lower lithosphere, or they could represent hybrids of such magmas produced by

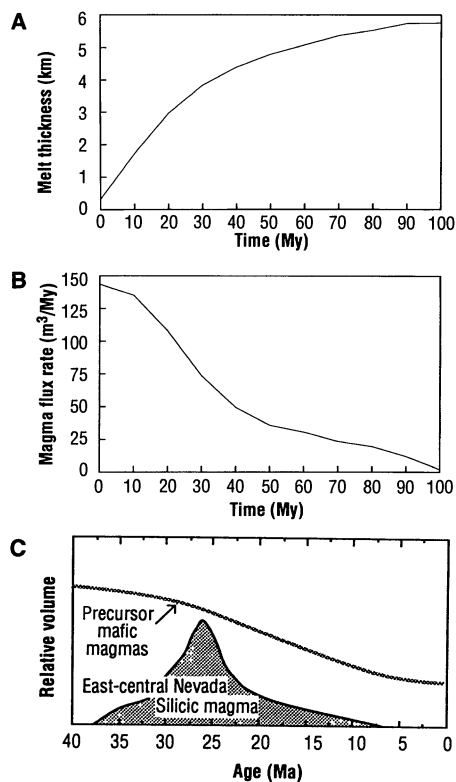
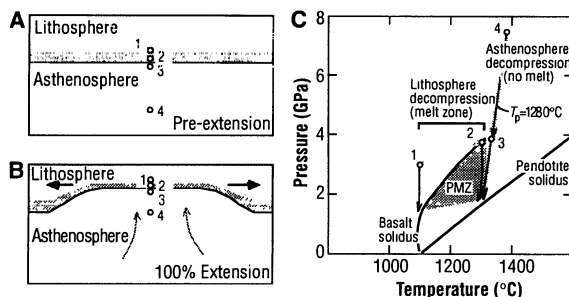


**Fig. 2.** Temporal variations in (A) the cumulative thickness of magma generated during extension and (B) the magma flux rate. We estimated the magma flux rate for a 1-km<sup>2</sup> region by taking the derivative of melt thickness with respect to time; it is assumed that melt is extracted instantaneously as it is generated. Calculated cumulative melt thickness is scaled by the percentage of the lower lithosphere composed of mafic material, in this case corresponding to 100% basaltic material; however, less than 10% of mafic material can account for actual extrusive volumes. Because we ignored changes in source composition with degree of melting, over time actual melt production would decrease more dramatically than depicted, and average melt composition would become increasingly more mafic. Magma generated in this way could have ultimately produced mid-Tertiary silicic magmas in the Great Basin after differentiation and crustal anatexis. (C) The pattern of silicic magma production in the east-central Nevada [from (14)] is broadly consistent with the modeled lithospheric melt production in (B). Formation of voluminous early mafic magma is inferred if crustal melting is driven by advective heating.

incorporation of crustal material.

We estimated the amount of magma produced by integrating the percentage of partial melt over the thickness of the lithosphere in the supersolidus field (Fig. 2A). For convenience, the magma production indicated in the figure corresponds to a lithospheric mantle composed of 100% mafic components and reaches a cumulative magma thickness of more than 5 km. As actual local thicknesses of volcanic rocks

**Fig. 3.** Schematic diagrams illustrating the binary source melting model. Hypothetical lithosphere sections are shown (A) before and (B) after 100% pure shear extension. Reference positions are indicated for mantle material at a point (1) above which no lithosphere melting is predicted (based on model in Fig. 1 and assuming dry melting of basalt), at points just above (2) and just below (3) the lithosphere-asthenosphere boundary (mechanical boundary layer), and at a point (4) in the asthenosphere twice as deep as the mechanical boundary layer. Decompression of these reference points after 100% extension is shown in P-T space in (C). Basaltic domains in lower lithosphere between (1) and (2) will melt to varying degrees (increasing toward the bottom of this layer), whereas peridotitic asthenosphere at (3) will only just approach melting conditions after ~100% extension. Deeper asthenospheric material [as at (4)] will still be well below the peridotite solidus after this degree of extension. PMZ is the partial melt zone for the model shown; continued extension and decompression will eventually lead to melting of asthenosphere, whereas melt production within the lower lithosphere will fall off dramatically because of its increasingly refractory character after extraction of initial melts.



within the Great Basin rarely exceed 0.5 km (14), the eruptive products could be related to melting lower lithospheric mantle containing ~10% of basaltic material. Still lower fractions of mafic components are required if eruptive centers draw laterally from melt generated over a broad region. However, considering that unknown amounts of magma were intruded into the crust, these estimates are considered to be minimal.

Under the conditions modeled, melt production begins virtually at the onset of extension and continues at a high rate for 10 My (Fig. 2B). Magma flux decreases rapidly between 10 and 40 My (20 to 40% extension) and decays gradually thereafter. This simple model reasonably simulates the volume-time pattern of extension-related magmatism inferred for the Great Basin from Oligocene to mid-Miocene time (Fig. 2C) (4, 14).

The demise of predominantly silicic magmatism and the appearance of voluminous basaltic magmas in the mid-Miocene marks a significant change in the magmatic record of the Great Basin. Isotopic and trace element compositions for the basaltic lavas apparently record a transition from lithospheric to asthenospheric magma sources from late Miocene to the present (38-42). This transition could reflect a change in tectonic style (that is, development of Basin and Range faulting) that favors more efficient eruption of waning melt contributions from the lower lithosphere. The timing of this transition is consistent with the mechanical aspects of extension and lithospheric thinning (30) if the potential temperature of the asthenosphere is slightly warmer (around 1340°C) than that assumed by McKenzie and Bickle (1). The combined effects of cooling of the lower lithosphere as it thins and its increas-

ingly refractory character as melt is extracted limit melt production in this part of the mantle during continued extension. In contrast, after ~100% lithospheric attenuation, upwelling asthenospheric mantle begins to melt, producing basalts compositionally similar to ocean island basalts (OIBs, Fig. 3). These magmas may ascend with little modification as they pass through the anhydrous, melt-depleted lower lithosphere. They may stagnate at crustal levels where silicic hybrid or anatectic magmas can form to produce the late Cenozoic bimodal basalt-rhyolite magmatism characteristic of the Basin and Range province (43). This phase of magmatism is conceptually similar to that described by McKenzie and Bickle (1), although the magmas produced differ in composition from ocean floor basalts. Leeman and Fitton (44) suggested that initial melts of asthenosphere may tap enriched veins or pods therein to produce OIB-like magmas, whereas more extensive melting (as beneath fully developed mid-ocean ridge spreading centers) eventually may tap relatively depleted matrix similar to sources for mid-ocean ridge basalts. Otherwise, rather complex compositionally layered structures must be invoked for the asthenosphere to explain the transition from typical rift magmatism to ocean ridge magmatism.

A two-layer, or binary source, model such as the one described here seems required to account for first-order details of timing and production rates of Great Basin extensional magmatism. Temporal compositional variations are also consistent with this type of model, but many geologic details and problems remain to be explained. Foremost are the cause for diachronous migration of magmatic fronts across the Great Basin (4) and the poor correspondence between loci of extension

and magmatism in some areas (14, 45). In detail, the heterogeneous nature of the lithosphere probably contributes to the observed complexity in volcanic and tectonic patterns.

## REFERENCES AND NOTES

- D. McKenzie and M. J. Bickle, *J. Petrol.* **25**, 713 (1988).
- D. M. Latin, J. E. Dixon, J. G. Fitton, N. White, in *Tectonic Events Responsible for Britain's Oil and Gas Reserves*, R. F. P. Hardman and J. Brooks, Eds. (Spec. Publ. 55, Geological Society of London, London, 1990), pp. 207–227.
- T. Pedersen and H. E. Ro, *Earth Planet. Sci. Lett.* **113**, 15 (1992).
- R. L. Armstrong and P. Ward, *J. Geophys. Res.* **96**, 13201 (1991); W. S. Snyder, W. R. Dickenson, M. L. Silberman, *Earth Planet. Sci. Lett.* **32**, 981 (1976).
- W. B. Hamilton, in *Metamorphism and Crustal Evolution of the Western United States*, W. G. Ernst, Ed. (Prentice-Hall, Englewood Cliffs, NJ, 1988), pp. 1–40.
- D. M. Miller, T. H. Nilsen, W. L. Bilodeau, in *The Cordilleran Orogen: Conterminous U.S.*, vol. G3, *The Geology of North America*, B. C. Burchfiel, P. W. Lipman, M. L. Zoback, Eds. (Geological Society of America, Boulder, CO, 1992), pp. 205–260.
- B. P. Wernicke, G. J. Axen, J. K. Snow, *Geol. Soc. Am. Bull.* **100**, 1738 (1988).
- N. L. Bogen and R. A. Schwieckert, *Earth Planet. Sci. Lett.* **75**, 93 (1985).
- R. E. Wells and P. L. Heller, *Geol. Soc. Am. Bull.* **100**, 325 (1988).
- N. Beghou and M. Barazangi, *Nature* **348**, 536 (1990).
- M. K. Savage, P. G. Silver, R. P. Meyer, *Geophys. Res. Lett.* **17**, 21 (1990).
- This statement excludes voluminous late Cenozoic hotspot-related magmatism of the Columbia River Plateau and Snake River Plain provinces that border the Great Basin to the north (17).
- P. B. Gans, G. A. Mahood, E. Schermer, *Geol. Soc. Am. Spec. Pap.* **233** (1989).
- M. G. Best and E. H. Christiansen, *J. Geophys. Res.* **96**, 13509 (1991).
- T. C. Feeley and A. L. Grunder, *Contrib. Mineral. Petrol.* **106**, 154 (1991).
- G. L. Farmer, D. E. Broxton, R. G. Warren, W. Pickthorn, *ibid.* **109**, 53 (1991).
- R. W. Carlson and W. K. Hart, *J. Geophys. Res.* **92**, 6121 (1987).
- R. L. Smith and R. G. Luedke, in *Explosive Volcanism: Inception, Evolution, and Hazards*, Geophysics Study Committee, Ed. (National Academy Press, Washington, DC, 1984), pp. 47–66.
- The later alkalic basalts closely resemble many oceanic island basalts in their trace element and isotopic characteristics, whereas compositions of the older tholeiitic basalts suggest they may be derived from distinct mantle sources, presumably within the lithosphere [J. G. Fitton, D. James, W. P. Leeman, *J. Geophys. Res.* **96**, 13593 (1991)]. This transition is diachronous in that true alkalic basalts erupted in the southern Great Basin only since ~5 Ma (38, 41, 42). In central Nevada they are uncommon and younger than 1 to 2 Ma [(39); C. C. Lum, thesis, Rice University, Houston (1992)]; none have been recognized in northern Nevada, Oregon, or Idaho. Although effects of crustal contamination cannot always be discounted, this pattern of compositional evolution suggests a change with time from initially lithospheric to asthenospheric sources in regions where alkalic basalts are present.
- M. A. Menzies, P. R. Kyle, M. Jones, G. Ingram, *J. Geophys. Res.* **96**, 13645 (1991).
- A. Nicolas, *J. Petrol.* **27**, 999 (1986).
- \_\_\_\_\_ and M. Jackson, *ibid.* **23**, 568 (1982).
- H. G. Wilshire, J. E. N. Pike, C. E. Meyer, E. L. Schwarzman, *Am. J. Sci.* **280-A**, 576 (1980); H. G. Wilshire *et al.*, *U.S. Geol. Surv. Prof. Pap.* **1443** (1988).
- D. L. Turcotte, *Annu. Rev. Earth Planet. Sci.* **10**, 397 (1982).
- B. S. Singer, J. D. Myers, S. R. Linneman, C. L. Angevine, *J. Volcanol. Geothermal Res.* **37**, 273 (1989).
- J. K. Meen, *Geol. Soc. Am. Spec. Pap.* **215** (1987), pp. 91–100.
- M. Wilson and H. Downes, *J. Petrol.* **32**, 811 (1991).
- D. McKenzie, *Earth Planet. Sci. Lett.* **40**, 25 (1978).
- Eq. 1 implies that volume is conserved during extension (28). In this model, the rate of lithospheric thinning decreases with time. An important consequence is that conductive cooling of the lower lithosphere is more pronounced at high degrees of extension, when the rate of lithospheric thinning is low.
- D. L. Harry, D. Sawyer, W. P. Leeman, *Earth Planet. Sci. Lett.* **117**, 59 (1993).
- M. Liu and C. G. Chase, *ibid.* **104**, 151 (1991).
- L. J. Sonder, P. C. England, B. P. Wernicke, R. L. Christiansen, in *Continental Extensional Tectonics*, M. P. Coward, J. F. Dewey, P. L. Hancock, Eds. (Spec. Publ. 28, Geological Society of London, London, 1987), pp. 187–201.
- Lamproitic magmas emplaced during the Eocene in the northern Rocky Mountains [F. O. Dudas, *J. Geophys. Res.* **96**, 13261 (1991); H. E. O'Brien, A. J. Irving, I. S. McCallum, *ibid.*, p. 13237] might be produced by such a process, but they are small in volume and compositionally dissimilar to volcanic rocks associated with mid-Tertiary extension (15, 17, 40).
- R. N. Thompson, *Contrib. Mineral. Petrol.* **52**, 213 (1975).
- J. R. Lister, *Earth Planet. Sci. Lett.* **107**, 233 (1991).
- P. B. Gans, *Tectonics* **6**, 1 (1987).
- Thompson's experiments (34) describe the solidus to liquidus phase relations in a typical olivine tholeiite from the Snake River Plain to pressures of 35 kbar. With his analyses of  $P_2O_5$  content in the experimental glasses, and assuming that phosphorus is not included in any solid phase, we calculated the fraction ( $F$ ) of glass (melt) for each analyzed experiment. The extent of melting was determined as a function of excess temperature above the solidus ( $T_{\text{excess}} = [T_{\text{experiment}} - T_{\text{solidus}}]/[T_{\text{liquidus}} - T_{\text{solidus}}]$ ) at the respective pressure of each experiment. The variables  $T_{\text{excess}}$  and  $F$  are linearly correlated, and their relation is expressed as  $F = 0.1703 + 0.7342 T_{\text{excess}}$ . The non-zero intercept is partly an artifact of the difficulties of detecting and analyzing small amounts of glass in runs used to define solidus temperatures.
- D. S. Ormerod, C. J. Hawkesworth, N. W. Rogers, W. P. Leeman, M. A. Menzies, *Nature* **333**, 349 (1988).
- C. C. Lum, W. P. Leeman, K. A. Foland, J. A. Kargel, J. G. Fitton, *J. Geophys. Res.* **94**, 7871 (1989).
- J. G. Fitton, D. James, W. P. Leeman, *ibid.* **96**, 13693 (1991); K. J. Fraser, C. J. Hawkesworth, A. J. Erlank, R. H. Mitchell, B. H. Scott-Smith, *Earth Planet. Sci. Lett.* **76**, 57 (1985).
- E. E. Daley and D. J. DePaolo, *Geology* **20**, 104 (1992).
- T. K. Bradshaw, C. J. Hawkesworth, K. Gallagher, *Earth Planet. Sci. Lett.* **116**, 45 (1993).
- R. L. Christiansen and P. W. Lipman, *Philos. Trans. R. Soc. London Ser. A* **271**, 249 (1972).
- W. P. Leeman and J. G. Fitton, *J. Geophys. Res.* **94**, 7682 (1989).
- G. J. Axen, W. J. Taylor, J. M. Bartley, *Geol. Soc. Am. Bull.* **105**, 56 (1993).
- T. J. Falloon and D. H. Green, *Earth Planet. Sci. Lett.* **94**, 364 (1989).
- B. Parsons and D. McKenzie, *J. Geophys. Res.* **83**, 4485 (1978).
- We thank J. Oldow and D. Sawyer for discussions about the modeling. Partially supported by NSF grant EAR90-18437 (W.P.L.).

19 July 1993; accepted 30 September 1993

## High- $T_C$ Molecular-Based Magnets: Ferrimagnetic Mixed-Valence Chromium(III)-Chromium(II) Cyanides with $T_C$ at 240 and 190 Kelvin

T. Mallah, S. Thiébaud, M. Verdaguer,\* P. Veillet

Molecular-based magnets with high magnetic-ordering temperatures,  $T_C$ , can be obtained by mild chemistry methods by focusing on the bimetallic and mixed-valence transition metal  $\mu$ -cyanide of the Prussian blue family. A simple orbital model was used to predict the electronic structure of the metal ions required to achieve a high ordering temperature. The synthesis and magnetic properties of two compounds,  $[Cr_6(CN)_{12}] \cdot 10H_2O$  and  $Cs_{0.75}[Cr_{2.125}(CN)_6] \cdot 5H_2O$ , which exhibited magnetic-ordering temperatures of 240 and 190 kelvin, respectively, are reported, together with the strategy for further work.

The synthesis of well-characterized molecular-based magnets with Curie temperatures,  $T_C$ 's, close to room temperature remains a challenge (1–4). We are trying to prepare molecular-based materials of low

density that are transparent and have a tunable high  $T_C$ .

For our work, the classical cyanide system, based on Prussian blue (5, 6), is particularly useful because (i) the synthesis of bimetallic or mixed-valence systems is easy and flexible, relying on the reaction of stable hexacyanometallates {octahedral  $[B(CN)_6]^{k-}$  Lewis bases, which can be used as molecular building blocks} with metallic cations  $A^{\ell+}$  (Lewis acids, used as assembling entities), where A and B can be transition metal ions with various oxidation

T. Mallah, S. Thiébaud, M. Verdaguer, Laboratoire de Chimie des Métaux de Transition, U.A. Centre National de la Recherche Scientifique 419, Université Pierre et Marie Curie, 4 Place Jussieu, 75252 Paris, France. P. Veillet, Institut d'Electronique Fondamentale, U.A. Centre National de la Recherche Scientifique 22, Université de Paris Sud, 91405 Orsay, France.

\*To whom correspondence should be addressed.